DIPARTIMENTO DI MATEMATICA
"Francesco Brioschi"
POLITECNICO DI MILANO

Hexagonal design for stiffening trusses

Gazzola, F.

Collezione dei *Quaderni di Dipartimento*, numero **QDD 143**
Inserito negli *Archivi Digitali di Dipartimento* in data 10-1-2013

Piazza Leonardo da Vinci, 32 - 20133 Milano (Italy)

Hexagonal design for stiffening trusses

Filippo GAZZOLA

Dipartimento di Matematica - Politecnico di Milano

Piazza Leonardo da Vinci 32 - 20133 Milano (Italy)

Abstract

We consider the problem of choosing the best design for stiffening trusses of plates, such as bridges. We suggest to cover the plate with regular hexagons which fit side to side. We show that this design has some important advantages when compared with alternative designs.

1 Introduction

The instability of certain bridges is still an unsolved problem. Classical mathematical theories such as [3] turned out to be too poor to describe the complex behavior of bridges, especially under the solicitation of strong and prolonged winds. Together with some colleagues, in [2, 9, 10] we have shown that most of the commonly adopted mathematical models fail and we could exhibit a phenomenon of self-excited oscillations in some semilinear fourth order ODE's. Moreover, this phenomenon is also visible in some fourth order PDE's arising from elasticity. We refer to [7] for a survey of the existing theories and for some historical events concerning the failure of bridges.

The purpose of the present paper is to suggest a new design for stiffening trusses to be put under the roadway of a bridge. In fact, our suggestion can be adapted to any structure having an horizontal plate to be sustained and to any kind of planking or scaffolding. Mathematically speaking, the problem consists in strengthening a plate $\Omega \subset \mathbb{R}^2$ with some trusses, identified with a line $\gamma \subset \Omega$. The truss is chosen to be the union of polygons P fitting side to side. The only regular polygons satisfying this property are equilateral triangles, squares and regular hexagons. Since most of the existing trusses are the union of isosceles right triangles (half squares cut along the diagonal) we also consider these shapes. We will show that regular hexagons have better performances from several different points of view.

Assuming that the surface X of the plate and the length L of the stiffening truss are given in advance, we first determine the number and the size of the polygons needed to cover the plate Ω. It turns out that the hexagonal covering has smallest segment of trusses (sides of the polygon), therefore being more resistant to moments of applied loads; recall that, for a given force, the moment is proportional to the distance from the fulcrum. Then we measure distances from uncovered points. As far as the minimal distance is involved, the four considered shapes perform equivalently; on one hand, this shows that symmetry plays an important role, on the other hand this claims a deeper analysis of the distances which should also take into account distance from *all* the points of the boundary. We introduce the *average mean squared distance*, a function of the L^2-norm of distances from the boundary. We prove that hexagonal trusses perform better also from this point of view since they minimize this value among the considered classes of polygons.

A further point of view comes from elasticity. We consider each polygon of the stiffening truss to be a simply supported elastic plate. Then, according to the linear theory of elasticity by von Kármán [18] (see also [13]), we can compute the elastic energy of the plate when it is subject to a constant load. This gives a measure of the *static performances* of each polygon. With the already computed optimal number of polygons, we are able to determine the total elastic energy of the plate Ω. It turns out that, again, hexagonal trusses perform better since they minimize the stored elastic energy.

Hence, our results suggest to cover plates as in Figure 1. This pattern may be repeated a number of times

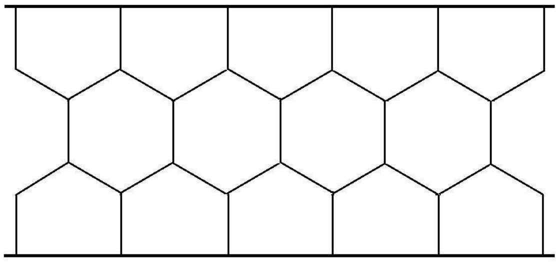

Figure 1: Optimal shape for stiffening trusses.

according to the given constraints (length and width of the plate).

This paper is organized as follows. In next section we describe in detail how to compute the parameters used to measure the performances of polygonal stiffening trusses and we state our main results. The results are stated by comparing the same parameter within the four classes of polygons, whereas in Section 3 the proofs are given by computing all the parameters for each considered polygon. Special mention deserves the result about the elastic performance, Theorem 4 stated in the next section. Due to the lack of explicit solutions, a full theoretical proof of this result is out of reach and, therefore, we take advantage of some numerics; this procedure is described in detail in Section 4. Finally, in Section 5 we draw some conclusions, summarizing and discussing all the results obtained.

2 Performances of polygonal stiffening trusses

We wish to reinforce a plate Ω of area X (computed in square meters, $|\Omega| = X\ m^2$) with a truss $\gamma \subset \Omega$ of total length L (computed in meters, $|\gamma| = L\ m$). Here γ is sought as a line in the plane which consists of a finite number of segments representing the sides of isosceles right triangles or equilateral triangles or squares or regular hexagons. We denote, respectively, by Θ, T, S, H these four classes of polygons and we assume that the stiffening truss gives rise to a design of several polygons all from the same class and all fitting side to side. By this we mean that the intersection between the closure of two polygons is either empty or one side or one vertex, see Figure 2.

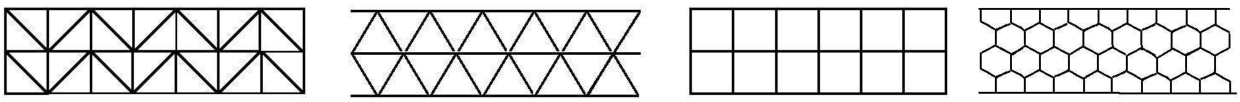

Figure 2: Polygonal shapes for stiffening trusses.

The model we have in mind is the roadway of a bridge and, therefore, the plate is a long and thin rectangle and L is very large when compared to $|\partial\Omega|$, $L \gg |\partial\Omega|$, so that one may neglect the contribution of $\partial\Omega$. To be slightly more precise, we assume that $L \approx 100|\partial\Omega|$ in such a way that the percentage of mistake is around 1%. This gives a reliable feeling on the behavior of plates reinforced with polygonal trusses.

We cover this plate with many small identical polygons P having one of the above described shapes and fitting side to side. The surface X of the plate and the length L of the truss determine both the *number* of the polygons P needed to cover the plate and their *size*. With a simple computation we obtain:

Theorem 1. *Let $\Omega \subset \mathbb{R}^2$ be a planar plate of area $|\Omega| = X$ strengthened with a truss $\gamma \subset \Omega$ of total length $|\gamma| = L$ with $L \gg |\partial\Omega|$. Assume that γ is the union of closed polygonal lines whose interior are all equal* *polygons P belonging to one of the above families, $P \in T \cup S \cup H \cup \Theta$. Assume that P has the sizes determined by X and L. Then the maximal length $\ell_{\max}(P)$ of one side of each polygon is given by*

P	Θ	T	S	H
$\ell_{\max}(P)$	$2(1+\sqrt{2}) \approx 4.83$	$2\sqrt{3} \approx 3.46$	2	$\frac{2\sqrt{3}}{3} \approx 1.15$

The quantities in this table should be multiplied by X/L and their unit of measure are meters.

Moreover, for any such shape, the number $N(P)$ of polygons needed to cover Ω is given by

P	Θ	T	S	H
$N(P)$	$(3-2\sqrt{2})\,\frac{L^2}{X}$	$\frac{\sqrt{3}}{9}\,\frac{L^2}{X}$	$\frac{1}{4}\,\frac{L^2}{X}$	$\frac{\sqrt{3}}{6}\,\frac{L^2}{X}$

In Theorem 1 we speak about *maximal length* of one side because for right triangles Θ the sides are not all equal; it is clear that for regular polygons in $T \cup P \cup H$ the maximal length is just the length of any side. For the second statement, what we call the *number* of polygons needs not be an integer, this depends on X and L; its integer part gives the "true" number of polygons, although the shape of Ω could force these polygons to be cut in a sophisticated way. Hence, the number $N(P)$ should be read as the approximation of a large integer number. Theorem 1 shows that a truss composed of hexagons has the minimal length of each segment truss. This gives better performances to the truss because shorter segments improve the performance to load solicitations due to a smaller moment of the force acting on it.

Once the sizes are determined, we introduce several further parameters in order to measure the performance of the truss. For any point $M \in P$ we consider the distance function from M to the boundary ∂P and we denote it by $d(M, \partial P)$; we emphasize that this function is, in fact, the *minimal distance from a point to the truss*:

$$d(M, \partial P) = \min_{A \in \partial P} d(M, A) = \min_{A \in \gamma} d(M, A) .$$

Then we define the **inradius** $I(P)$ as the radius of the largest disk contained in P; this represents the *maximal distance from the truss to a point* of P and is analytically defined by

$$I(P) = \max_{M \in P} d(M, \partial P) = \|d(\cdot, \partial P)\|_{L^\infty(P)} .$$

This number is a further parameter characterizing the polygon P: the larger is $I(P)$ the weaker is the stiffening truss. We also consider the **average distance** $\overline{d}(P)$ from points of P to trusses which can be defined by

$$\overline{d}(P) = \frac{1}{|P|} \int_P d(M, \partial P)\, dM = \frac{1}{|P|} \|d(\cdot, \partial P)\|_{L^1(P)} .$$

Moreover, the **variance** of the distance to γ is given by

$$V(P) = \int_\Omega \Big(d(M, \gamma) - \overline{d}(P) \Big)^2 dM \tag{1}$$

and measures how heterogeneous is the distance function from the truss γ. It is clear that the larger is $V(P)$, the weaker appears the structure since it has larger gaps between "weak" and "strong" points. In fact, for the four above considered shapes, these three parameters are identical.

Theorem 2. *Let $\Omega \subset \mathbb{R}^2$ be a planar plate of area $|\Omega| = X$ strengthened with a truss $\gamma \subset \Omega$ of total length $|\gamma| = L$ with $L \gg |\partial\Omega|$. Assume that γ is the union of closed polygonal lines whose interior are all equal polygons P belonging to one of the above families, $P \in T \cup S \cup H \cup \Theta$. Assume that P has the sizes determined by Theorem 1. Let $I(P)$, $\overline{d}(P)$, $V(P)$ be as just defined. Then, for any such shape, we have*

$$I(P) = \frac{X}{L} , \qquad \overline{d}(P) = \frac{1}{3}\,\frac{X}{L} , \qquad V(P) = \frac{1}{18}\,\frac{X^3}{L^2} .$$

Theorem 2 may appear surprising, none of the four considered shapes performs better than the others, at least from a first analysis of the distance to the boundary. We do not know how general this result can be, which other shapes enjoy this property. For sure, it does not hold for rectangles (see Section 5.1) and, presumably, for any irregular polygon. Most probably it merely holds for *circumscribed domains* which fit side to side.

Since from the *minimal distance* point of view, the four polygonal shapes are completely equivalent, we introduce a further parameter going deeper into distances from the boundary; it does not only take into account the minimal distance from $M \in P$ to ∂P but also the distance from M to *any* point in ∂P. In Figure 3 the

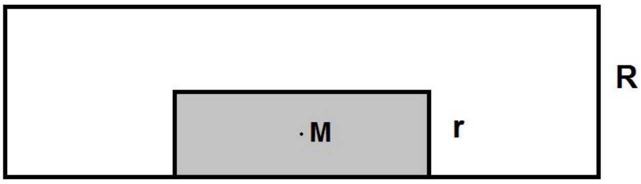

Figure 3: A point having the same minimal distance from two different boundaries.

point M has the same (minimal) distance from the boundaries of the large white rectangle R and the small grey rectangle r. However, by the maximum principle applied to problem (3) below, if a load f is put in M then the simply supported plate r will be deformed less than the plate R. So, for every point $M \in P$ we first define the *mean squared distance* by

$$\delta(M) = \frac{1}{|\partial P|} \left(\int_{\partial P} d(M,A)^2 \, dA \right)^{1/2}$$

and then we define the **average mean squared distance** of the polygon P by

$$\Delta(P) = \frac{1}{|P|} \int_P \frac{1}{|\partial P|^2} \int_{\partial P} d(M,A)^2 \, dA \, dM = \frac{1}{|P|} \|\delta\|^2_{L^2(P)} \,. \tag{2}$$

In Section 5.2 we explain the meaning of this new measure for performances of trusses. Here, we state

Theorem 3. *Let $\Omega \subset \mathbb{R}^2$ be a planar plate of area $|\Omega| = X$ strengthened with a truss $\gamma \subset \Omega$ of total length $|\gamma| = L$ with $L \gg |\partial\Omega|$. Assume that γ is the union of closed polygonal lines whose interior are all equal polygons P belonging to one of the above families, $P \in T \cup S \cup H \cup \Theta$. Assume that P has the sizes determined by Theorem 1. Then, for any such shape, the average mean squared distance $\Delta(P)$ is given by*

P	Θ	T	S	H
$\Delta(P)$	$\frac{1}{3} \approx 0.333$	$\frac{\sqrt{3}}{6} \approx 0.289$	$\frac{1}{4} = 0.25$	$\frac{5\sqrt{3}}{36} \approx 0.241$

The quantities in this table should be multiplied by X/L and their unit of measure are meters.

We believe that any L^p-norm (for $1 \le p < \infty$) would give the same qualitative answer. More precisely, for any such p one could consider the mean value of the p-th power of the distance

$$\frac{1}{|P|} \int_P \frac{1}{|\partial P|^p} \int_{\partial P} d(M,A)^p \, dA \, dM$$

and, presumably, obtain a result similar to Theorem 3 with hexagons having the best performance.

Finally, we study the different trusses from the point of view of elasticity. For small vertical displacements, the elastic performances of simply supported plates can be computed by using the linear theory by von Kármán [18], see also [8, 11] for a modern approach and for further historical references. Adopting this theory, the vertical deformation u of a simply supported planar elastic plate $\Omega \subset \mathbb{R}^2$ subject to an external force (load) $f \in L^2(\Omega)$ is described by the equation

$$\begin{cases} \Delta^2 u = f & \text{in } \Omega \\ u = \Delta u = 0 & \text{on } \partial\Omega\ . \end{cases} \tag{3}$$

Note that (3) may be written as a system of two second order equations

$$\begin{cases} -\Delta v = f & \text{in } \Omega \\ v = 0 & \text{on } \partial\Omega\ , \end{cases} \qquad \begin{cases} -\Delta u = v & \text{in } \Omega \\ u = 0 & \text{on } \partial\Omega\ . \end{cases} \tag{4}$$

It is well-known that (3) admits a unique solution $\overline{u} \in \mathcal{H} := H^2 \cap H^1_0(\Omega)$ which may also be obtained as the unique minimizer of the convex functional

$$J(u) = \int_\Omega \left(\frac{|\Delta u|^2}{2} - f\, u \right) \qquad u \in \mathcal{H}\ .$$

Then the elastic energy of the deformed plate under the solicitation f is given by

$$\mathcal{E}_f(\Omega) = -2 \min_{u \in \mathcal{H}} J(u) = -2J(\overline{u}) = \int_\Omega |\Delta \overline{u}|^2$$

where the last equality is obtained by multiplying (3) by $\overline{u}$ and integrating by parts over Ω.

Of particular interest is the situation when $f \equiv 1$ (constant load). This gives a reliable measure of the elastic energy storing capacity of the plate per unit load. In this situation, the elastic energy is homogeneous of degree 6 under dilations:

$$\mathcal{E}(\alpha\Omega) = \alpha^6 \mathcal{E}(\Omega) \qquad \forall \alpha > 0\ . \tag{5}$$

Moreover, in view of (4), when $f \equiv 1$ the elastic energy becomes

$$\mathcal{E}(\Omega) = \int_\Omega |\Delta \overline{u}|^2 = \int_\Omega \overline{v}^2 \tag{6}$$

where $\overline{v} \in H^1_0(\Omega)$ is the unique solution to the *torsion problem*

$$\begin{cases} -\Delta v = 1 & \text{in } \Omega \\ v = 0 & \text{on } \partial\Omega\ . \end{cases} \tag{7}$$

Except for some particular shapes, equation (7) is not explicitly solvable. However, with the help of some numerics we obtain

Theorem 4. (Partially numerical results) *Let $\Omega \subset \mathbb{R}^2$ be a planar plate of area $|\Omega| = X$ strengthened with a truss $\gamma \subset \Omega$ of total length $|\gamma| = L$ with $L \gg |\partial\Omega|$. Assume that γ is the union of closed polygonal lines whose interior are all equal polygons P belonging to one of the above families, $P \in T \cup S \cup H \cup \Theta$. Assume that P has the sizes determined by Theorem 1. Then, for any such shape, the total elastic energy of the plate Ω under the action of a unitary load is given by*

P	Θ	T	S	H
$\mathcal{E}(P)$	≈ 0.034	$\frac{9}{280} \approx 0.032$	≈ 0.027	≈ 0.024

The quantities in this table should be multiplied by X^5/L^4.

Hence, also from this point of view regular hexagons perform better than the other shapes.

3 Proof of Theorems 1 – 2 – 3

For each of the four shapes P considered we fix the length of one side and we determine several characteristic parameters:
- their perimeter $|\partial P|$;
- their area $|P|$;
- their inradius $I(P)$ (the maximal distance from a point in P and the boundary ∂P);
- the number $N(P)$ of polygons P needed to cover a plate Ω with area X (computed in square meters, $|\Omega| = X\,m^2$) and with total length of the truss L (computed in meters, $|\gamma| = L\,m$);
- the average distance of their points from the boundary $\overline{d}(P)$;
- the size of the $N(P)$ polygons, in particular $\ell_{\max}(P)$;
- the variance of the distance $V(P)$ as defined in (1);
- the average mean squared distance $\Delta(P)$ as defined in (2).

These parameters enable us to compute the performances of the trusses having the shape considered. In order to determine $N(P)$ and the size of P we need to solve the following equation

$$N(P) = \frac{X}{|P|} = \frac{2L}{|\partial P|}\,. \tag{8}$$

The factor 2 in the right hand side of (8) is needed since each side of any polygon P is also the side of an adjacent polygon, so the contribution of each polygon to the truss γ is $|\partial P|/2$.

Another parameter requiring some work is the average distance $\overline{d}$. Since the distance function to ∂P is the simplest example of *web function* (see [6]) we may use the *piercing function* defined in [4] and compute $\overline{d}$ according to [5, Lemma 4]. Given an arbitrary convex planar domain K, for a.e. $y \in \partial K$ the outer unit normal is well-defined and will be denoted by n_y. For all $x \in K$ let $d(x, \partial K)$ denote its distance from the boundary ∂K, and define its projection on the boundary $\Pi(x) \in \partial K$ such that $|x - \Pi(x)| = d(x, \partial K)$; note that $\Pi(x)$ is uniquely determined for a.e. $x \in K$. The piercing function is defined as

$$\lambda_K(y) := \sup\{k \geq 0 \,:\, \Pi(y - kn_y) = y\} \qquad \text{for a.e. } y \in \partial K. \tag{9}$$

We clearly have $0 \leq \lambda_K(y) \leq I(K)$ on ∂K. Moreover, the function λ_K is Lipschitz continuous on ∂K whereas Π is Lipschitz continuous on $\overline{K}$.

A relatively simple way to compute integrals of functions of the distance d_P over a convex polygon P is given in [5, Lemma 4] which states

Lemma 5. *Let P be a convex polygon of inradius $I(P)$, and let $g : [0, I(P)] \to \mathbb{R}$ be a Lipschitz continuous function such that $g(0) = 0$. Then*

$$\int_{\partial P} g(\lambda_P(y))\,dy = \int_P g'\Big(d(x, \partial P)\Big)\,dx\,.$$

In particular, by taking $g(s) = s^q$ we have

$$\int_P d(x, \partial P)^{q-1}\,dx = \frac{1}{q}\int_{\partial P} \lambda_P(y)^q\,dy\,. \tag{10}$$

For the computation of the integrals of the distance, we make use of (10) with $q = 2$ and $q = 3$. To this end, we need to clarify how to determine λ_P; this is quite simple since our polygons are all *circumscribed* to some disk, more involved is the general case, see [4]. Put one of the sides of the polygon on a segment Σ of equal length on the x axis in the (x, y)-plane so that P lies in the half space $y > 0$. Construct the inner bisecting lines of the two vertices of P at the endpoints of Σ and stop them when they intersect. We obtain a triangle having the side Σ on the x axis and the remaining two sides being the graph of a piecewise affine function defined on Σ. This is the graph of λ_P for the points belonging to the segment Σ.

Concerning the variance of the distance *within each polygon* P, we will proceed as follows:

$$\int_P d(x,\partial P)^2\,dx - 2\overline{d}(P)\int_P d(x,\partial P)\,dx + |P|\,\overline{d}(P)^2 = \int_P d(x,\partial P)^2\,dx - |P|\,\overline{d}(P)^2\,; \tag{11}$$

then, recalling the definition in (1) and the number of polygons in (8), we obtain the total variance as

$$V(P) = N(P)\left(\int_P d(x,\partial P)^2\,dx - |P|\,\overline{d}(P)^2\right)\,. \tag{12}$$

Finally, for the average mean squared distance

$$\Delta(P) = \frac{1}{|P|}\int_P \frac{1}{|\partial P|^2}\int_{\partial P} d(M,A)^2\,dA\,dM = \frac{1}{|P|\cdot|\partial P|^2}\int_P\int_{\partial P} d(M,A)^2\,dA\,dM$$

we will simplify computations by exploiting the symmetry properties of each polygon P. We are now ready to determine the characteristic values of the considered convex polygons.

3.1 Isosceles right triangles

Consider an isosceles right triangle Θ_ℓ whose hypothenuse has length 2ℓ. Then

$$|\partial\Theta_\ell| = 2(1+\sqrt{2})\ell\,,\quad |\Theta_\ell| = \ell^2\,,\quad I(\Theta_\ell) = (\sqrt{2}-1)\,\ell\,. \tag{13}$$

Hence, by using (8) we obtain

$$N(\Theta_\ell) = \frac{X}{\ell^2} = \frac{L}{(1+\sqrt{2})\ell} \implies \ell = (1+\sqrt{2})\,\frac{X}{L} \implies N(\Theta_\ell) = (3-2\sqrt{2})\,\frac{L^2}{X}\,. \tag{14}$$

In the plane (x,y) put first the hypothenuse h on the axis $y=0$ with $-\ell < x < \ell$ so that Θ_ℓ lies in the half plane $y>0$. For any $x \in (-\ell,\ell)$ we have

$$\lambda_{\Theta_\ell}(x) = \min\left\{(\sqrt{2}-1)(\ell-x), (\sqrt{2}-1)(\ell+x)\right\}\,.$$

For symmetry reasons, we only need to compute the contribution of λ_{Θ_ℓ} on the interval $(0,\ell)$ and to multiply it by 2 since there are 2 identical right triangles which compose the lower part of Θ_ℓ, see the first picture in Figure 4. This gives

$$\int_h \lambda_{\Theta_\ell}(x)^2\,dx = 2(\sqrt{2}-1)^2\int_0^\ell (\ell-x)^2\,dx = \frac{2(\sqrt{2}-1)^2}{3}\,\ell^3\,. \tag{15}$$

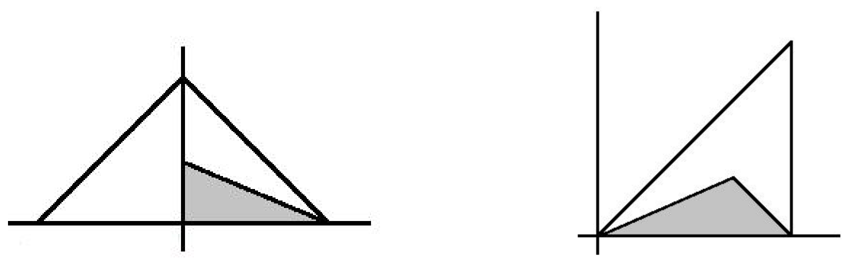

Figure 4: Contributions of the piercing function in Θ_ℓ.

Then put one of the legs on the axis $y = 0$ with $0 < x < \sqrt{2}\ell$ so that Θ_ℓ lies in the half plane $y > 0$, see the second picture in Figure 4. In view of $\tan\frac{\pi}{8} = \sqrt{2} - 1$, for any $x \in (0, \sqrt{2}\ell)$ we have

$$\lambda_{\Theta_\ell}(x) = \min\left\{(\sqrt{2}-1)x, \sqrt{2}\ell - x\right\} .$$

Since we have 2 legs c_1 and c_2, we double the contribution of λ_{Θ_ℓ} on the interval $(0, \sqrt{2}\ell)$. This gives

$$\int_{c_1\cup c_2} \lambda_{\Theta_\ell}(x)^2\,dx = 2\left\{(\sqrt{2}-1)^2\int_0^\ell x^2\,dx + \int_\ell^{\sqrt{2}\ell}(\sqrt{2}\ell - x)^2\,dx\right\} = \frac{2\sqrt{2}(\sqrt{2}-1)^2}{3}\,\ell^3 . \tag{16}$$

By adding (15)-(16) and by using (10) with $q = 2$ we obtain

$$\int_{\Theta_\ell} d(M, \partial\Theta_\ell)\,dM = \frac{\sqrt{2}-1}{3}\,\ell^3 .$$

With the value of ℓ determined in (14) we can compute, in terms of X and L, the maximal and the average distance of points inside Θ_ℓ from the boundary $\partial\Theta_\ell$:

$$I(\Theta_\ell) = \frac{X}{L} , \qquad \overline{d}(\Theta_\ell) = \frac{1}{|\Theta_\ell|}\int_{\Theta_\ell} d(M, \partial\Theta_\ell)\,dM = \frac{\sqrt{2}-1}{3}\,\ell = \frac{1}{3}\,\frac{X}{L} . \tag{17}$$

Let us now compute the variance of the distance within each triangle. By using (10) with $q = 3$ and by arguing as above we get

$$\begin{aligned}\int_{\Theta_\ell} d(M, \partial\Theta_\ell)^2\,dM &= \frac{2}{3}(\sqrt{2}-1)^3\int_0^\ell(\ell - x)^3\,dx + \frac{2}{3}\left\{(\sqrt{2}-1)^3\int_0^\ell x^3\,dx + \int_\ell^{\sqrt{2}\ell}(\sqrt{2}\ell - x)^3\,dx\right\}\\ &= \frac{3-2\sqrt{2}}{6}\,\ell^4 .\end{aligned}$$

Hence, by (17) and (11),

$$\int_{\Theta_\ell}\Big(d(M, \partial\Theta_\ell) - \overline{d}(\Theta_\ell)\Big)^2\,dM = \frac{3-2\sqrt{2}}{6}\,\ell^4 - \frac{3-2\sqrt{2}}{9}\,\ell^4 = \frac{3-2\sqrt{2}}{18}\,\ell^4 .$$

By using the number of triangles and their optimal side length determined in (14), by (12) we find

$$V(\Theta) = \frac{1}{18}\,\frac{X^3}{L^2} .$$

Let now Θ_ℓ be the isosceles right triangle delimited by the lines $y = 0$, $x = 0$, $y = \sqrt{2}\ell - x$. Then the three sides of Θ_ℓ have the parametric representations

$$r_1(t) = (t, 0) , \quad r_2(t) = (0, t) , \quad r_3(t) = (t, \lambda - t) , \qquad (0 \le t \le \lambda)$$

where we have set $\lambda = \sqrt{2}\,\ell$. For all $M(x, y) \in T_\ell$, we have

$$\int_{\partial\Theta_\ell} d(M, \sigma)^2\,d\sigma = \sum_{i=1}^{3}\int_0^\lambda d(M, r_i(t))^2\,dt$$

and, for symmetry reasons, we have

$$\Delta(\Theta_\ell) = \frac{1}{|\Theta_\ell|\cdot|\partial\Theta_\ell|^2}\int_{\Theta_\ell}\int_{\partial\Theta_\ell} d(M, A)^2\,dA\,dM$$

$$= \frac{1}{4(1+\sqrt{2})^2\,\ell^4} \int_{\Theta_\ell} \int_0^\lambda [2d(M, r_1(t))^2 + d(M, r_3(t))]\,dt\,dM\ , \tag{18}$$

where we used (13). Note first that

$$\int_0^\lambda d(M, r_1(t))^2\,dt = \int_0^\lambda [(t-x)^2 + y^2]\,dt = \frac{1}{3}\,\lambda^3 + \lambda(x^2+y^2) - \lambda^2 x\ .$$

This quantity has to be integrated over Θ_ℓ:

$$\int_{\Theta_\ell} \left[\frac{1}{3}\,\lambda^3 + \lambda(x^2+y^2) - \lambda^2 x\right] dydx$$

$$= \frac{1}{3}\,\lambda^3\,|\Theta_\ell| + \lambda \int_0^\lambda \int_0^{\lambda - x} [x^2 + y^2 - \lambda x]\,dy\,dx = \frac{\lambda^5}{6} = \frac{2\sqrt{2}}{3}\,\ell^5\ . \tag{19}$$

Then we rotate Θ_ℓ in order to have the hypothenuse r_3 coinciding with the segment $[-\ell, \ell] \times \{0\}$ and with Θ_ℓ being contained in the half plane $y > 0$; we compute

$$\int_{r_3} d(M, \sigma)^2\,d\sigma = \frac{2}{3}\,\ell^3 + 2\ell(x^2+y^2)\ .$$

This quantity has to be integrated over Θ_ℓ and, by symmetry reasons, we obtain

$$\int_{\Theta_\ell} \left[\frac{2}{3}\,\ell^3 + 2\ell(x^2+y^2)\right] dydx$$

$$= \frac{2}{3}\,\ell^3\,|\Theta_\ell| + 4\ell \int_0^\ell \int_0^{\ell - x} [x^2+y^2]\,dy\,dx = \frac{4}{3}\,\ell^5\ . \tag{20}$$

By inserting (19)-(20) into (18) we obtain

$$\Delta(\Theta_\ell) = \frac{1}{4(1+\sqrt{2})^2\,\ell^4} \left(\frac{4\sqrt{2}}{3}\,\ell^5 + \frac{4}{3}\,\ell^5\right) = \frac{\ell}{3(\sqrt{2}+1)} = \frac{1}{3}\,\frac{X}{L}$$

where we used (14).

3.2 Equilateral triangles

Consider an equilateral triangle T_ℓ whose sides have length ℓ. Then

$$|\partial T_\ell| = 3\ell\ , \quad |T_\ell| = \frac{\sqrt{3}}{4}\,\ell^2\ , \quad I(T_\ell) = \frac{\sqrt{3}}{6}\,\ell\ .$$

Hence, by using (8) we obtain

$$N(T_\ell) = \frac{4X}{\sqrt{3}\ell^2} = \frac{2L}{3\ell} \implies \ell = 2\sqrt{3}\,\frac{X}{L} \implies N(T_\ell) = \frac{\sqrt{3}}{9}\,\frac{L^2}{X}\ . \tag{21}$$

In the plane (x, y) put one side of T_ℓ on the axis $y = 0$ with $-\frac{\ell}{2} < x < \frac{\ell}{2}$ so that T_ℓ lies in the half plane $y > 0$. For any $x \in (-\frac{\ell}{2}, \frac{\ell}{2})$ we have

$$\lambda_{T_\ell}(x) = \min\left\{\frac{1}{\sqrt{3}}\Big(\frac{\ell}{2} - x\Big), \frac{1}{\sqrt{3}}\Big(\frac{\ell}{2} + x\Big)\right\}\ .$$

For symmetry reasons, we only need to compute the contribution of λ_{T_ℓ} on the interval $(0, \ell/2)$ and to multiply it by 6 since there are 6 identical right triangles which compose T_ℓ. Hence, by using (10) with $q = 2$ we obtain

$$\int_{T_\ell} d(M, \partial T_\ell)\, dM = \int_0^{\ell/2} \Big(\frac{\ell}{2} - x\Big)^2 dx = \frac{1}{24}\,\ell^3\,.$$

With the value of ℓ determined in (21) we can compute, in terms of X and L, the maximal and the average distance of points inside T_ℓ from the boundary ∂T_ℓ:

$$I(T_\ell) = \frac{X}{L}\,, \qquad \overline{d}(T_\ell) = \frac{1}{|T_\ell|}\int_{T_\ell} d(M, \partial T_\ell)\, dM = \frac{\sqrt{3}}{18}\,\ell = \frac{1}{3}\,\frac{X}{L}\,. \tag{22}$$

Let us now compute the variance of the distance within each triangle. By using (10) with $q = 3$ and by arguing as above we get

$$\int_{T_\ell} d(M, \partial T_\ell)^2\, dM = \frac{1}{3}\int_{\partial T_\ell} \lambda_{T_\ell}(y)^3\, dy = \frac{2\sqrt{3}}{9}\int_0^{\ell/2} \Big(\frac{\ell}{2} - x\Big)^3 dx = \frac{\sqrt{3}}{288}\,\ell^4\,.$$

Hence, by (22) and (11),

$$\int_{T_\ell} \Big(d(M, \partial T_\ell) - \overline{d}(T_\ell)\Big)^2 dM = \frac{\sqrt{3}}{288}\,\ell^4 - \frac{\sqrt{3}}{432}\,\ell^4 = \frac{\sqrt{3}}{864}\,\ell^4\,.$$

By using the number of triangles and their optimal side length determined in (21), by (12) we find

$$V(T) = \frac{1}{18}\,\frac{X^3}{L^2}\,.$$

Let now T_ℓ be the equilateral triangle delimited by the lines $y = 0$, $y = \sqrt{3}(x + \frac{\ell}{2})$, $y = \sqrt{3}(\frac{\ell}{2} - x)$. Then the basis of T_ℓ has the parametric representation

$$r_1(t) = \left(t - \frac{\ell}{2}, 0\right) \qquad (0 \le t \le \ell)$$

while the remaining two sides have parametric representations $r_i = r_i(t)$ for $i = 2, 3$ and $0 \le t \le \ell$. For all $M(x, y) \in T_\ell$, we have

$$\int_{\partial T_\ell} d(M, \sigma)^2\, d\sigma = \sum_{i=1}^{3} \int_0^\ell d(M, r_i(t))^2\, dt$$

and, for symmetry reasons, we have

$$\Delta(T_\ell) = \frac{1}{|T_\ell| \cdot |\partial T_\ell|^2}\int_{T_\ell}\int_{\partial T_\ell} d(M, A)^2\, dA\, dM = \frac{4\sqrt{3}}{9\,\ell^4}\int_{T_\ell}\int_0^\ell d(M, r_1(t))^2\, dt\, dM\,, \tag{23}$$

the number $\frac{4\sqrt{3}}{9\,\ell^4}$ being obtained by multiplying by 3 the inverse of the measures.

For simplicity, we put $\lambda = \ell/2$; then, since the integrand is even,

$$\int_0^\ell d(M, r_1(t))^2\, dt = 2\int_0^\lambda [t^2 + x^2 + y^2]\, dt = \frac{2}{3}\,\lambda^3 + 2\lambda(x^2 + y^2)\,.$$

This quantity has to be integrated over T_ℓ; by symmetry we may only integrate over half of T_ℓ, the part in the half plane $x > 0$:

$$\int_{T_\ell} \left[\frac{2}{3}\,\lambda^3 + 2\lambda(x^2 + y^2)\right] dy\, dx$$

$$= \frac{2}{3}\,\lambda^3\,|T_\ell| + 4\lambda\int_0^\lambda\int_0^{\sqrt{3}(\lambda - x)} [x^2 + y^2]\, dy\, dx = \frac{\sqrt{3}}{16}\,\ell^5\,.$$

By inserting this into (23) and recalling (21) we obtain

$$\Delta(T_\ell) = \frac{1}{12}\,\ell = \frac{\sqrt{3}}{6}\,\frac{X}{L} \approx 0.289\,\frac{X}{L}\,.$$

3.3 Squares

Consider a square S_ℓ whose sides have length ℓ. Then

$$|\partial S_\ell| = 4\ell\ , \quad |S_\ell| = \ell^2\ , \quad I(S_\ell) = \frac{\ell}{2}\ .$$

Hence, by using (8), we obtain

$$N(S_\ell) = \frac{X}{\ell^2} = \frac{L}{2\ell} \implies \ell = 2\,\frac{X}{L} \implies N(S_\ell) = \frac{1}{4}\,\frac{L^2}{X}\ . \tag{24}$$

In the plane (x, y) assume that $S_\ell = (0, \ell)^2$; then, for any $x \in (0, \ell)$, we have

$$\lambda_{S_\ell}(x) = \min\{x, \ell - x\}\ .$$

For symmetry reasons, we only need to compute the contribution of λ_{S_ℓ} on the interval $(0, \ell/2)$ and to multiply it by 8 since there are 8 identical right triangles which compose S_ℓ. Hence, by using (10) with $q = 2$ we obtain

$$\int_{S_\ell} d(M, \partial S_\ell)\, dM = 4 \int_0^{\ell/2} x^2\, dx = \frac{1}{6}\,\ell^3\ .$$

With the value of ℓ determined in (24) we can compute, in terms of X and L, the maximal and the average distance of points inside S_ℓ from the boundary ∂S_ℓ:

$$I(S_\ell) = \frac{X}{L}\ , \qquad \overline{d}(S_\ell) = \frac{1}{|S_\ell|} \int_{S_\ell} d(M, \partial S_\ell)\, dM = \frac{1}{6}\,\ell = \frac{1}{3}\,\frac{X}{L}\ . \tag{25}$$

Let us now compute the variance of the distance within each square. By using (10) with $q = 3$ and by arguing as above we get

$$\int_{S_\ell} d(M, \partial S_\ell)^2\, dM = \frac{1}{3} \int_{\partial S_\ell} \lambda_{S_\ell}(y)^3\, dy = \frac{8}{3} \int_0^{\ell/2} x^3\, dx = \frac{1}{24}\,\ell^4\ .$$

Hence, by (25) and (11),

$$\int_{S_\ell} \Big(d(M, \partial S_\ell) - \overline{d}(S_\ell)\Big)^2\, dM = \frac{1}{24}\,\ell^4 - \frac{1}{36}\,\ell^4 = \frac{1}{72}\,\ell^4\ .$$

By using the number of triangles and their optimal side length determined in (21), by (12) we find

$$V(S) = \frac{1}{18}\,\frac{X^3}{L^2}\ .$$

Consider again $S_\ell = (0, \ell)^2$ and let $r_i = r_i(t)$ be the parametric representations of the 4 sides of S_ℓ with $t \in (0, \ell)$. For all $M(x, y) \in S_\ell$, we have

$$\int_{\partial S_\ell} d(M, \sigma)^2\, d\sigma = \sum_{i=1}^{4} \int_0^\ell d(M, r_i(t))^2\, dt$$

and, for symmetry reasons, we have

$$\Delta(S_\ell) = \frac{1}{|S_\ell| \cdot |\partial S_\ell|^2} \int_{S_\ell} \int_{\partial S_\ell} d(M, A)^2\, dA\, dM = \frac{1}{4\,\ell^4} \int_{S_\ell} \int_0^\ell d(M, r_1(t))^2\, dt\, dM\ , \tag{26}$$

the number $\frac{1}{4\,\ell^4}$ being obtained by multiplying by 4 the inverse of the measures $\frac{1}{16\,\ell^4}$.

With no loss of generality we may take $r_1(t) = (t, 0)$ for $0 \le t \le \ell$ so that

$$\int_0^\ell d(M, r_1(t))^2\, dt = \int_0^\ell [(t-x)^2 + y^2]\, dt = \ell y^2 + \ell x^2 - \ell^2 x + \frac{\ell^3}{3} .$$

This quantity has to be integrated over S_ℓ:

$$\int_{S_\ell} \left[\ell y^2 + \ell x^2 - \ell^2 x + \frac{\ell^3}{3}\right] dx\, dy = \frac{\ell^5}{2} .$$

By replacing into (26) and by recalling (24), we then obtain

$$\Delta(S_\ell) = \frac{\ell}{8} = \frac{1}{4}\frac{X}{L} .$$

3.4 Hexagons

Consider a regular hexagon H_ℓ whose sides have length ℓ. Then

$$|\partial H_\ell| = 6\ell , \quad |H_\ell| = \frac{3\sqrt{3}}{2}\,\ell^2 , \quad I(H_\ell) = \frac{\sqrt{3}}{2}\,\ell .$$

Hence, by using (8) we obtain

$$N(H_\ell) = \frac{2X}{3\sqrt{3}\ell^2} = \frac{L}{3\ell} \implies \ell = \frac{2\sqrt{3}}{3}\frac{X}{L} \implies N(H_\ell) = \frac{\sqrt{3}}{6}\frac{L^2}{X} . \tag{27}$$

In the plane (x, y) put one side of H_ℓ on the axis $y = 0$ with $-\frac{\ell}{2} < x < \frac{\ell}{2}$ so that H_ℓ lies in the half plane $y > 0$. For any $x \in (-\frac{\ell}{2}, \frac{\ell}{2})$ we have

$$\lambda_{H_\ell}(x) = \min\left\{\sqrt{3}\Big(\frac{\ell}{2} - x\Big), \sqrt{3}\Big(\frac{\ell}{2} + x\Big)\right\} .$$

For symmetry reasons, we only need to compute the contribution of λ_{H_ℓ} on the interval $(0, \ell/2)$ and to multiply it by 12 since there are 12 identical right triangles which compose H_ℓ. Hence, by using (10) with $q = 2$ we obtain

$$\int_{H_\ell} d(M, \partial H_\ell)\, dM = 18 \int_0^{\ell/2} \Big(\frac{\ell}{2} - x\Big)^2 dx = \frac{3}{4}\,\ell^3 .$$

With the value of ℓ determined in (27) we can compute, in terms of X and L, the maximal and the average distance of points inside H_ℓ from the boundary ∂H_ℓ:

$$I(H_\ell) = \frac{X}{L} , \qquad \overline{d}(H_\ell) = \frac{1}{|H_\ell|}\int_{H_\ell} d(M, \partial H_\ell)\, dM = \frac{\sqrt{3}}{6}\,\ell = \frac{1}{3}\frac{X}{L} . \tag{28}$$

Let us now compute the variance of the distance within each hexagon. By using (10) with $q = 3$ and by arguing as above we get

$$\int_{H_\ell} d(M, \partial H_\ell)^2\, dM = \frac{1}{3}\int_{\partial H_\ell} \lambda_{H_\ell}(y)^3\, dy = 12\sqrt{3}\int_0^{\ell/2} \Big(\frac{\ell}{2} - x\Big)^3 dx = \frac{3\sqrt{3}}{16}\,\ell^4 .$$

Hence, by (28) and (11),

$$\int_{H_\ell} \Big(d(M, \partial H_\ell) - \overline{d}(H_\ell)\Big)^2 dM = \frac{3\sqrt{3}}{16}\,\ell^4 - \frac{\sqrt{3}}{8}\,\ell^4 = \frac{\sqrt{3}}{16}\,\ell^4 .$$

By using the number of triangles and their optimal side length determined in (21), by (12) we find

$$V(S) = \frac{1}{18}\,\frac{X^3}{L^2}\ .$$

Consider again the regular hexagon H_ℓ lying entirely in the half plane $y > 0$ and having one side coinciding with the segment

$$r_1(t) = \left(t - \frac{\ell}{2}, 0\right)\ , \qquad (0 \le t \le \ell)\ ;$$

the remaining 5 sides have parametric representations $r_i = r_i(t)$ for all $i = 2, 3, 4, 5, 6$ and for $0 \le t \le \ell$. For all $M(x, y) \in H_\ell$, we have

$$\int_{\partial H_\ell} d(M,\sigma)^2\, d\sigma = \sum_{i=1}^{6} \int_0^\ell d(M, r_i(t))^2\, dt$$

and, for symmetry reasons, we have

$$\Delta(H_\ell) = \frac{1}{|H_\ell| \cdot |\partial H_\ell|^2} \int_{H_\ell} \int_{\partial H_\ell} d(M, A)^2\, dA\, dM = \frac{\sqrt{3}}{27\,\ell^4} \int_{H_\ell} \int_0^\ell d(M, r_1(t))^2\, dt\, dM\ , \tag{29}$$

the number $\frac{\sqrt{3}}{27\,\ell^4}$ being obtained by multiplying by 6 the inverse of the measures. For simplicity, we put $\lambda = \ell/2$; then, since the integrand is even,

$$\int_0^\ell d(M, r_1(t))^2\, dt = 2 \int_0^\lambda [t^2 + x^2 + y^2]\, dt = \frac{2}{3}\,\lambda^3 + 2\lambda(x^2 + y^2)\ .$$

This quantity has to be integrated over H_ℓ; by symmetry we may only integrate over half of H_ℓ, the part in the half plane $x > 0$:

$$\int_{H_\ell} \left[\frac{2}{3}\,\lambda^3 + 2\lambda(x^2 + y^2)\right] dydx$$

$$= \frac{2}{3}\,\lambda^3\,|H_\ell| + 4\lambda \int_0^\lambda \int_0^{2\sqrt{3}\lambda} [x^2 + y^2]\, dy\, dx + 4\lambda \int_\lambda^{2\lambda} \int_{\sqrt{3}(x-\lambda)}^{\sqrt{3}(3\lambda - x)} [x^2 + y^2]\, dy\, dx = \frac{15\sqrt{3}}{8}\,\ell^5\ .$$

By inserting this into (29) and recalling (27) we obtain

$$\Delta(H_\ell) = \frac{5}{24}\,\ell = \frac{5\sqrt{3}}{36}\,\frac{X}{L} \approx 0.241\,\frac{X}{L}\ .$$

4 Elastic energy of polygons: numerical results and proof of Theorem 4

This section is divided into several subsections. In Subsection 4.1 we make a by-hand computation of the value of $\mathcal{E}(T)$; this may be used to evaluate the precision of our numerical results. In Subsection 4.2 we give a theoretical proof (no numerics at all!) that regular hexagons perform better than equilateral triangles. In Subsection 4.3 we explain our numerical procedure and we give the numerical results obtained for the four shapes $\Theta \cup T \cup S \cup H$.

4.1 Exact value for equilateral triangles

Consider the equilateral triangle T in the (x, y)-plane delimited by the three lines

$$y = 0\ , \quad y = \sqrt{3}(1 - x)\ , \quad y = \sqrt{3}(1 + x)\ ,$$

so that its sides have length 2. When $\Omega = T$ it is well-known that the solution to the torsion problem (7) may be obtained by multiplying the equations representing the three sides:

$$\overline{v}(x,y) = \frac{1}{4\sqrt{3}}(y^3 - 2\sqrt{3}\,y^2 - 3\,x^2y + 3\,y)\ .$$

Then, according to (6) and by exploiting the symmetry properties of T and $\overline{v}$, we have

$$\mathcal{E}(T) = \int_T \overline{v}^2 = 2\int_0^1 \int_0^{\sqrt{3}(1-x)} \overline{v}(x,y)\,dy\,dx = \frac{\sqrt{3}}{280}\ .$$

By (21) we know that the optimal side of the equilateral triangle T_ℓ is $\ell = 2\sqrt{3}\,\frac{X}{L}$. By recalling (5) we then obtain

$$\mathcal{E}(T_\ell) = \mathcal{E}\left(\sqrt{3}\,\frac{X}{L}\,T\right) = \left(\sqrt{3}\,\frac{X}{L}\right)^6 \mathcal{E}(T) = \frac{27\sqrt{3}}{280}\,\frac{X^6}{L^6} \approx 0.167\,\frac{X^6}{L^6}\ .$$

Finally, since by (21) we have $N(T_\ell) = \frac{\sqrt{3}}{9}\,\frac{L^2}{X}$, we infer that the total elastic energy $\mathcal{E}(T)$ is given by

$$\mathcal{E}(T) = \frac{9}{280}\,\frac{X^5}{L^4} \approx 0.032\,\frac{X^5}{L^4}\ . \tag{30}$$

4.2 Theoretical proof that regular hexagons perform better than equilateral triangles

If $\Omega = D_R$, the disk of radius R centered at the origin, then (7) admits the unique solution

$$\overline{v}(x,y) = \frac{R^2 - x^2 - y^2}{4}$$

and the elastic energy (6) is easily computed to be

$$\mathcal{E}(B_R) = \frac{\pi}{48}\,R^6\ .$$

Now take a regular hexagon H_ℓ having sides of length ℓ. Then the inscribed disk has radius $\rho_1 = \frac{\sqrt{3}}{2}\ell$ and, by the maximum principle for (7),

$$\mathcal{E}(H_\ell) > \mathcal{E}(D_{\rho_1}) = \frac{9\pi}{1024}\,\ell^6\ .$$

Consider now the disk having the same measure as H_ℓ; its radius ρ_2 satisfies $\pi\rho_2^2 = \frac{3\sqrt{3}}{2}\ell^2$. By Talenti's comparison principle [16, Theorem 1] and by classical results in symmetrization theory, we have

$$\mathcal{E}(H_\ell) < \mathcal{E}(D_{\rho_2}) = \frac{27\sqrt{3}}{128\pi^2}\,\ell^6\ .$$

By taking into account the optimal length ℓ and the needed number of hexagons $N(H_\ell)$ found in (27), we infer that the total elastic energy $\mathcal{E}(H)$ satisfies the bounds

$$0.0189\,\frac{X^5}{L^4} \approx \frac{\pi\sqrt{3}}{288}\,\frac{X^5}{L^4} < \mathcal{E}(H) < \frac{1}{4\pi^2}\,\frac{X^5}{L^4} \approx 0.0253\,\frac{X^5}{L^4}\ . \tag{31}$$

This gives a *purely theoretical* proof that $\mathcal{E}(H) < \mathcal{E}(T)$, see (30).

4.3 Numerical values for right triangles, squares and hexagons

If $\Omega = S_\ell = (0,\ell)^2 \subset \mathbb{R}^2$ (a square with sides of length ℓ in the (x,y)-plane) then, by separating variables, one may find the "explicit" solution to (7):

$$\begin{aligned}\overline{v}(x,y) &= -\frac{x^2}{2} + \ell^2 \sum_{n=1}^{\infty} \frac{1-(-1)^n}{n\pi \sinh(n\pi)} \sinh\Big(\frac{n\pi x}{\ell}\Big) \sin\Big(\frac{n\pi y}{\ell}\Big) \\ &\quad + \ell^2 \sum_{n=1}^{\infty} \frac{2(-1)^n - 2 - n^2\pi^2(-1)^n}{n^3\pi^3 \sinh(n\pi)} \sin\Big(\frac{n\pi x}{\ell}\Big) \left[\sinh\Big(\frac{n\pi(\ell-y)}{\ell}\Big) + \sinh\Big(\frac{n\pi y}{\ell}\Big)\right] .\end{aligned}$$

But, of course, the exact value of $\int_{S_\ell} \overline{v}^2$ cannot be computed by hand. In general, the torsion problem on polygons is widely studied from several points of view [14, 15]. However, for right triangles and hexagons the explicit solution to (7) is not known and we may only proceed numerically.

We used the PDE Toolbox of Matlab in order to have an approximation v_0 of the solution $\overline{v}$ to (7). Once the plot of v_0 was performed we exported both the vector containing the values of v_0 in the nodes of the mesh and the mesh itself. With an ad-hoc program we computed the squared L^2-norm of v_0: we exploited the fact that v_0^2 is a polynomial of degree 2 on each triangle of the mesh and therefore its norm may be computed by taking the average of its values in the three midpoints of the sides of the triangle. We tested the numerical results in two different ways. First, we tried them in the case of equilateral triangles and disks where the solution to (7) is explicitly known, see Sections 4.1 and 4.2. Second, we selected finer meshes to check if the results were "stable". In the below table we quote the results so obtained for a right triangle $\Theta_{\sqrt{2}}$ having hypothenuse of length $2\sqrt{2}$, for a square S_1 having side of length 1, for an hexagon H_1 having side of length 1.

P	$\Theta_{\sqrt{2}}$	S_1	H_1
$\mathcal{E}(P)$	0.0079	0.0017	0.0348

These numbers have to be scaled according to the sizes found in Theorem 1, see (14)-(24)-(27); we obtain

$$\mathcal{E}(\Theta_\ell) \approx 0.1955\, \frac{X^6}{L^6} \qquad \mathcal{E}(S_\ell) \approx 0.1088\, \frac{X^6}{L^6} \qquad \mathcal{E}(H_\ell) \approx 0.0825\, \frac{X^6}{L^6} .$$

In turn, these numbers have to be multiplied, respectively, by $N(\Theta_\ell)$-$N(S_\ell)$-$N(H_\ell)$, see again (14)-(24)-(27); in such a way we obtain the values appearing in the Table in Theorem 4. In particular, we obtain $\mathcal{E}(H) \approx 0.024\, \frac{X^5}{L^4}$ which should be compared with (31).

5 Further remarks and conclusions

5.1 Performances of rectangles

Consider a rectangle R_ℓ whose sides have length ℓ and $\gamma\ell$ with $\gamma > 1$. Then

$$|\partial R_\ell| = 2(\gamma+1)\ell\ , \quad |R_\ell| = \gamma\ell^2\ , \quad I(R_\ell) = \frac{\ell}{2}\ .$$

Hence, by using (8), we obtain

$$N(R_\ell) = \frac{X}{\gamma\ell^2} = \frac{L}{(\gamma+1)\ell} \implies \ell = \frac{\gamma+1}{\gamma}\,\frac{X}{L} \implies N(R_\ell) = \frac{\gamma}{(\gamma+1)^2}\,\frac{L^2}{X}\ . \tag{32}$$

Hence, $\ell_{\max}(R) = (\gamma+1)\frac{X}{L}$; this number should be compared with the values in the second table of Theorem 1. In particular, it appears that $\ell_{\max}$ is increasing with respect to the ratio between the two sides,

Figure 5: Regions for piercing functions in a rectangle.

elongated rectangles have large $\ell_{\max}$ and, therefore, bad resistance to the moments of forces; this is the weak point of rectangles.

Since R_ℓ is not circumscribed to a disk, the piercing function is slightly more involved. For a detailed description we refer to [4], here we explain how to proceed by referring to Figure 5.

In the plane (x, y) put the short side of R_ℓ on the axis $y = 0$ with $0 < x < \ell$ so that R_ℓ lies in the half plane $y > 0$. For any $x \in (0, \ell)$ we have

$$\lambda_{R_\ell}(x) = \min\{x, \ell - x\} \ .$$

For symmetry reasons, we only need to compute the contribution of λ_{R_ℓ} on the interval $(0, \ell/2)$ and to multiply it by 8 since the 8 identical grey right triangles which compose R_ℓ give the same contribution, see Figure 5. Moreover, if we put the long side of R_ℓ on the axis $y = 0$, we find the 2 white rectangles in Figure 5 which give the same constant contribution in terms of the piercing function, $\lambda_R(x) = \frac{\ell}{2}$. Summarizing, by using (10) with $q = 2$ we obtain

$$\int_{R_\ell} d(M, \partial R_\ell)\, dM = 4 \int_0^{\ell/2} x^2\, dx + \int_0^{(\gamma-1)\ell} \frac{\ell^2}{4}\, dx = \frac{3\gamma - 1}{12}\, \ell^3 \ .$$

With the value of ℓ determined in (32) we compute, in terms of X and L, the maximal and the average distance of points inside R_ℓ from the boundary ∂R_ℓ:

$$I(R_\ell) = \frac{\gamma + 1}{2\gamma}\, \frac{X}{L}\ , \qquad \overline{d}(R_\ell) = \frac{1}{|R_\ell|} \int_{R_\ell} d(M, \partial R_\ell)\, dM = \frac{3\gamma - 1}{12\gamma}\, \ell = \frac{(3\gamma - 1)(\gamma + 1)}{12\gamma^2}\, \frac{X}{L}\ . \tag{33}$$

Let us now compute the variance of the distance within each rectangle. By using (10) with $q = 3$ and by arguing as above we get

$$\int_{R_\ell} d(M, \partial R_\ell)^2\, dM = \frac{1}{3} \int_{\partial R_\ell} \lambda_{R_\ell}(y)^3\, dy = \frac{8}{3} \int_0^{\ell/2} x^3\, dx + \frac{2}{3} \int_0^{(\gamma-1)\ell} \frac{\ell^3}{8}\, dx = \frac{2\gamma - 1}{24}\, \ell^4\ .$$

Hence, by (33) and (11),

$$\int_{R_\ell} \Big(d(M, \partial R_\ell) - \overline{d}(R_\ell)\Big)^2\, dM = \frac{3\gamma^2 - 1}{144\gamma}\, \ell^4\ .$$

Finally, by using the number of rectangles and their optimal side length determined in (32), by (12) we find

$$V(R) = \frac{(\gamma + 1)^2 (3\gamma^2 - 1)}{144\gamma^4}\, \frac{X^3}{L^2}\ .$$

Concerning the average mean squared distance, by repeating the above computations, we find

$$\Delta(R) = \frac{4\gamma^3 - \gamma^2 + 2\gamma + 1}{12(\gamma + 1)^2}\, \ell = \frac{4\gamma^3 - \gamma^2 + 2\gamma + 1}{12\gamma(\gamma + 1)}\, \frac{X}{L}\ ;$$

we see that, again, $\Delta(R)$ is increasing with respect to the ratio γ between the two sides, yielding worse performances.

5.2 What is the average mean squared distance

Take the disk D of radius 1 and centered at the origin O. Then the mean squared distance from O to ∂D is $\delta(O) = 1/\sqrt{2\pi}$. Take now a point on the boundary, for instance $A(1,0)$. Then the mean squared distance from A to ∂D may be computed as

$$\delta(A) = \frac{1}{2\pi}\left(\int_0^{2\pi}[(1-\cos(t))^2+\sin^2(t)]\,dt\right)^{1/2} = \frac{1}{\sqrt{\pi}} > \frac{1}{\sqrt{2\pi}} = \delta(O).$$

Hence, $A \in \partial D$ has mean distance from ∂D larger than the mean distance from the center O to ∂D.

Take a square S having sides of length 1. Then there are 8 half sides of S which have squared distance $t^2 + \frac{1}{4}$ from its barycenter B for $t \in [0, \frac{1}{2}]$; hence, the mean squared distance from B to ∂S is given by

$$\delta(B) = \frac{1}{4}\left(8\int_0^{1/2}\left[t^2+\frac{1}{4}\right]dt\right)^{1/2} = \frac{\sqrt{3}}{6}\,.$$

If we consider a vertex V, then the points on the 2 two adjacent sides of S have a squared distance t^2 from V for $t \in [0,1]$ while the points on the two opposite sides of S have a squared distance t^2+1 from V for $t \in [0,1]$. Summarizing, the mean squared distance from V to ∂S is

$$\delta(V) = \frac{1}{4}\left(\int_0^1 (4t^2+2)\,dt\right)^{1/2} = \frac{\sqrt{30}}{12} > \frac{\sqrt{3}}{6} = \delta(B)\,.$$

Again, $V \in \partial S$ has mean squared distance from ∂S larger than the mean squared distance from the barycenter B to ∂S.

These two examples highlight the role of the mean squared distance. It evaluates how homogeneous are distances from the boundary to points of the polygon: the barycenter of the polygon has a smaller value since its distances from the boundary are "almost constant" while points close to the boundary have a larger value since they are far away from other parts of the boundary. Hence, the mean squared distance should be seen as a "measure of homogeneity" explaining how different can be the action of the same load put in different points of the plate. But the purpose of $\Delta(P)$ is not to analyze the competition between different points of the same polygon; since it is the average of this homogeneity measure, it appears suitable for comparing performances between different shapes. Basically, it gives an average of the homogeneity between different points; by comparing this average for different shapes one has an additional parameter measuring the performances. Larger values of $\Delta(P)$ give worse performances as can be easily understood by noticing the homogeneity with respect to dilations: $\Delta(\alpha P) = \alpha\Delta(P)$ for all $\alpha > 0$ and, of course, αP is weaker than P if $\alpha > 1$.

5.3 Concluding remarks

We introduced several parameters in order to measure the performances of polygonal stiffening trusses for a given plate Ω. It appears that hexagonal trusses perform better under different points of view. First of all, they have the least largest sides among the polygons considered, see Theorem 1: this means that each segment of the truss is more resistant to moments of forces due to applied loads. In particular, in order to solve the dilemma between economy and stiffness (see [12]) one could use *thinner* trusses segments in case of hexagonal shapes. Second, we proved that the minimal distance to the boundary and its variance are the same for all the shapes considered, see Theorem 2. This suggested to introduce a new parameter measuring the effect of distances from the boundary, what we called average mean squared distance, see the description in Section 5.2. Also for this parameter, the best performances are obtained by hexagonal trusses, see Theorem 3. Finally, we measured numerically the stored elastic energy for the shapes under observation; Theorem 4 states that hexagonal trusses store the least energy.

Although the first project of a suspension bridge is due to the Italian engineer Verantius around 1615, see [17] and [12, p.16], the first suspension bridges were built only about two centuries later in Great Britain. Samuel Brown (1776-1852) was an early pioneer of suspension bridge design and construction. He is best known for the Union Bridge of 1820, the first vehicular suspension bridge in Britain. According to [1],

The invention of the suspension bridges by Sir Samuel Brown sprung from the sight of a spider's web hanging across the path of the inventor, observed on a morning's walk, when his mind was occupied with the idea of bridging the Tweed.

The results obtained in this paper suggest that

when thinking about how to strengthen a suspension bridge, one should observe a bee hive.

References

[1] C. Bender, *Historical sketch of the successive improvements in suspension bridges to the present time*, American Soc. Civil Eng. Vol. I, 27-43 (1872)

[2] E. Berchio, A. Ferrero, F. Gazzola, P. Karageorgis, *Qualitative behavior of global solutions to some nonlinear fourth order differential equations*, J. Diff. Eq. **251**, 2696-2727 (2011)

[3] F. Bleich, C.B. McCullough, R. Rosecrans, G.S. Vincent, *The mathematical theory of vibration in suspension bridges*, U.S. Dept. of Commerce, Bureau of Public Roads, Washington D.C. (1950)

[4] G. Crasta, I. Fragalà, F. Gazzola, *A sharp upper bound for the torsional rigidity of rods by means of web functions*, Arch. Rat. Mech. Anal. **164**, 189-211 (2002)

[5] G. Crasta, I. Fragalà, F. Gazzola, *Some estimates of the torsional rigidity of composite rods*, Math. Nachr. **280**, 242-255 (2007)

[6] F. Gazzola, *Existence of minima for nonconvex functionals in spaces of functions depending on the distance from the boundary*, Arch. Rat. Mech. Anal. **150**, 57-76 (1999)

[7] F. Gazzola, *Nonlinearity in oscillating bridges*, preprint

[8] F. Gazzola, H.-Ch. Grunau, G. Sweers, *Polyharmonic boundary value problems*, LNM **1991**, Springer (2010)

[9] F. Gazzola, R. Pavani, *Blow up oscillating solutions to some nonlinear fourth order differential equations*, Nonlinear Analysis **74**, 6696-6711 (2011)

[10] F. Gazzola, R. Pavani, *Wide oscillations finite time blow up for solutions to nonlinear fourth order differential equations*, to appear in Arch. Rat. Mech. Anal.

[11] F. Gazzola, G. Sweers, *On positivity for the biharmonic operator under Steklov boundary conditions*, Arch. Rat. Mech. Anal. **188**, 399-427 (2008)

[12] T. Kawada, *History of the modern suspension bridge: solving the dilemma between economy and stiffness*, ASCE Press (2010)

[13] E.H. Mansfield, *The bending and stretching of plates*, 2nd Edition, Cambridge Univ. Press (2005)

[14] P.M. Quinlan, *The torsion of an irregular polygon*, Proc. Roy. Soc. London (Series A, Mathematical and Physical Sciences) **282**, 208-227 (1964)

[15] B.R. Seth, *Torsion of beams whose cross-section is a regular polygon of n sides*, Math. Proc. Cambridge Philos. Soc. **30**, 139-149 (1934)

[16] G. Talenti, *Elliptic equations and rearrangements*, Ann. Scuola Norm. Sup. Pisa Cl. Sci. **3**, 697-718 (1976)

[17] F. Verantius, *Machinae novae*, 1615

[18] T. von Kármán, *Feestigkeitsprobleme in maschinenbau*, In: Encycl. der Mathematischen Wissenschaften, Vol. IV/4C, 348-352, F. Klein & C. Müller (Editors), Leipzig (1910)